Influence of Microcrystalline Wax on the Properties of Model Wax-Oil Gels

Muh Kurniawan[1,2], Sreedhar Subramanian[1], Jens Norrman[1], Kristofer Paso[1]

1 Ugelstad Laboratory, Department of Chemical engineering, Norwegian University of Science and Technology, NO-7491, Trondheim, Norway.

2 LEMIGAS, Research and Development Centre for Oil and Gas Technology, Jakarta, Indonesia

ABSTRACT

The influence of micro-crystalline wax addition upon the rheological properties of model wax-oil gels is investigated. Addition of less than 1 wt% micro-crystalline wax to a model oil consisting of 5 wt% macro-crystalline wax in dodecane shows no significant impact on the WAT and gelation temperature. Beyond 1 wt% added micro-crystalline wax, increases in WAT and gelation temperature are observed, and are attributable to the higher crystallization temperature of the micro-crystalline wax. The effect of micro-crystalline wax addition upon the WAT and gelation temperature are shown to be attributed to merely overlapping compositions of macro- and micro-crystalline wax. However, a substantive effect of micro-crystalline wax addition is observed on the yield stress. Addition of 0.13 wt% micro-crystalline wax reduces the yield stress of waxy oil model from 238.0 to 22.5 Pa. Addition of 0.5 wt% micro-crystalline wax decreases the yield stress to 5.4 Pa, which is close in value to the yield stress of neat 5 wt% micro-crystalline wax gel.

Microscopic images reveal two mechanisms leading to formation of a weak mixed wax gels. At low to medium addition of micro-crystalline wax, micro-crystalline crystallites formed during cooling provide nucleation sites for subsequent precipitation of macro-crystalline wax. Macro-crystalline wax crystals formed in contact with micro-crystalline crystallites are smaller in size and the growth is localized, in comparison to neat macro-crystalline wax. Modified macro-crystalline wax precipitation leads to uneven dispersion of the macro-crystalline crystals in the liquid phase. At high concentration, micro-crystals form throughout the sample prior to precipitation of macro-crystalline wax. Hence, only small and discrete space remains for macro-crystalline crystals to grow, forming small crystals. Interlocking among macro-crystals is spatially hindered by the presence of micro-crystalline crystallites. In this condition, the system completely behaves as a micro-crystalline gel. This investigation provides a plausible mechanistic account for the known gel weakening activity of micro-crystalline wax.

INTRODUCTION

Wax present in petroleum fluids gives rise to a variety of well-known problems within the petroleum industry, primarily attributed to the solubility of wax in petroleum fluids, which is strongly dependent on the temperature of the system as well as the composition and architecture of the wax. At reservoir condition, wax is generally soluble in petroleum fluids. However, wax solubility decreases as temperature is reduced during various production stages. Below the cloud point, long alkanes precipitate out of the fluid and form solid wax crystals. Depending on the type of petroleum fluid, the composition of the wax may range from predominantly low molecular weight n-alkanes to large fractions of high molecular weight iso-alkanes and cyclic

alkanes [1]. The former type of wax is termed macro-crystalline wax, while the latter type is termed micro-crystalline wax.

Owing to the linear molecular structure, n-alkanes in macro-crystalline wax tend to form large plate-like crystals. Macro-crystalline wax isolated from crude oil consist primarily of a distribution of carbon numbers from approximately C_{20} to C_{40}. On the other hand, branched and cyclic alkane tend to form solids with lower degree of crystallinity. Solids formed from branched and cyclic alkanes are more amorphous in nature and have a tendency to not grow into large size particles. As it generally forms smaller particles than macro-crystalline wax, this type of wax is generally referred to as micro-crystalline wax, even though it consists of predominantly larger molecules, with the branched and cyclic components generally within the carbon number range of approximately C_{30}-C_{70+}. Physically, the two different types of paraffin waxes, macro-crystalline wax and micro-crystalline wax, show stark differences in several properties. Macro-crystalline wax is translucent, glossy, slick, and brittle, while micro-crystalline wax is more opaque, plastic, malleable, and sticky.

Flow assurance problems in waxy oil production and transport operations are often, but not always, associated with macro-crystalline wax. Precipitation of wax crystals significantly increases crude oil viscosity and gradually changes the flow properties of the crude oil from pure viscous behavior to non-Newtonian behavior. The crude oil begins to show non-Newtonian flow behavior at a temperature somewhat below the wax appearance temperature (WAT).

Upon further cooling, additional wax crystals precipitate out and interlock with each other to form a three dimensional macrostructure. This process occurs rapidly under quiescent conditions associated with flow outages. Substantial amounts of liquid may be occluded in the three

dimensional network structure of wax crystals [2]. The result of this occlusion process is gelation of the crude oil and a concomitant loss of fluidity. Various research [1, 3-5] has shown that as little as 1-6 wt% precipitated wax is sufficient to cause oil gelling. The physical state of a waxy oil gel and the relevant rheological properties are strictly determined by the mode of particle aggregation and the spatial distribution and coordination of aggregates [6]. As an elastic gel is formed, stress must be applied to the system before it starts to yield and flow again. The shear stress at the point of gel fracture is defined as the yield stress [7]. The yield stress of a wax gel depends on its composition, thermal history, and shear history [8-9].

Macro-crystalline wax crystals contain a distribution of carbon numbers. n-alkane molecules that are close to the same length can readily packed together in the same crystal, so-called co-crystallization. For long n-alkanes (longer than C_{28}), Dirand et.al found that in solid wax melts, molecules with four carbon chain difference are partially or completely miscible [10]. In order to account for the packing of different molecule sizes in the same crystal structure, Dirand proposed a structure molecule conformation defect [10], while Dorset proposed a model of super-lattice [11]. In wax solutions, where solvent is incorporated into the system, n-alkanes are capable of cocrystallizing with one another and forming multicomponent solid solutions [12].

In addition to causing problems in oil transportation, especially in high pour point crudes, micro-crystalline wax is also known to contribute strongly to the formation of tank-bottom sludges. Micro-crystalline wax is extracted from heavy distillates and used in a broad range of applications which include cosmetics, rubber compounds, candles, and metal casting to utilize its specific flexibility, viscosity, temperature resistance, and adhesive qualities.

There is not much literature available on the role of micro-crystalline wax in relation to flow assurance. Garcia et al. found that waxes extracted from various Venezuelan crude oils can be n-paraffin rich as well as iso-paraffin rich [13]. Dorset et al. investigated the crystal packing of pure iso-paraffins [14] and real waxes [15] and found that pendant branches can be accommodated within gaps provided by chain ends at adjacent lamellae. Paso suggested an indication that branched and cyclic paraffin components have an inhibiting effect on the formation of strong wax-gels from the linear paraffin components [8]. Zhao et al. showed that strength of micro-crystalline wax gel is much lower than that of macro-crystalline wax [16]. Bacon et al. statistically demonstrated that micro-crystalline wax exhibits a less elongated crystal size and shape in comparison to macro-crystalline wax; and a chemical treatment effectively inhibited wax crystal growth for both wax types [17]. Garcia et al. found that the effect of cyclic and branched alkanes on the activity of a commercial crystal modifier was complex. At low to medium concentrations, the effect was antagonistic, while an enhancing effect was observed at concentrations of cyclo + branched alkanes greater than 50 wt% [18].

The work presented in the current article is an investigation on effect of micro-crystalline wax on model wax-oil gels formed under quiescent and near-quiescent cooling conditions. The article covers the crystal precipitation properties as well as gelation and rheological yield behavior. Microscopic observation of crystal morphologies provides additional insight into the observed precipitation, gelation, and rheological behavior.

EXPERIMENTAL SECTION

Materials

Macro-crystalline wax (Sasolwax 5405) and micro-crystalline wax (Sasolwax 3971) were obtained from Sasol Wax GmbH. Both waxes were used as received without any further treatment. The compositional data is obtained by high temperature gas chromatography, and was performed by Sasol Wax GmbH using a proprietary HTGC protocol. The Sasolwax 5405 consists of 78 wt% linear paraffins in the carbon number range C_{22}-C_{44} and 22 wt% non-linear paraffins in the carbon number range C_{20}-C_{41}. The Sasolwax 3971 consists of 16 wt% linear paraffins in the carbon number range C_{22}-C_{58} and 84 wt% non-linear paraffins in the carbon number range C_{25}-C_{80}.

The solvent used was n-dodecane ReagentPlus® solvent grade with purity >99 wt% obtained from Sigma Aldrich. Waxy model oil were prepared by dissolving the appropriate amount of wax in dodecane.

Differential Scanning Calorimetry (DSC)

DSC experiments were performed using a DSC Q-2000 from TA Instruments equipped with TZero system. The instrument was calibrated with Indium, and aluminium hermetically sealed pans were used in order to prevent mass loss during sample heating.

Prior to loading into a DSC pan, wax solutions were heated to 80 °C and maintained at 80 °C temperature for at least 2 hours in order to ensure homogeneity. 10-15 mg of sample was filled into the pan and the pan was hermitically sealed with a lid. The experimental cooling protocol consisted of equilibrating the sample at 80°C for 10 minutes, followed by a cooling ramp to -20°C at rate of 1°C min^{-1}. Data acquisition and processing were performed using TA Instrument software. All DSC measurements are repeated in triplicate in order to confirm experimental reproducibility.

Rheology

An Anton Paar Physica MCR 301 Rheometer was used for the rheological experiments. The rheometer was fitted with 2° cone and plate geometry of 4 cm diameter and gap of 57 μm. In order to reduce slippage effects, the contact surface of the cone was previously roughened using sand blasting. A Peltier plate in thermal communication with the fluid sample provides temperature control.

Wax solution was preheated on a hot plate maintained at 300°C for 15 minutes in closed container. The hot plate was subsequently cooled to 150°C and maintained for at least 2 hours before starting the test. This pre-treatment serves ensures that the sample state is in a homogenous liquid phase, while simultaneously preventing evaporation during the high temperature pre-treatment stage.

Gelation Temperature Determination

Sample was loaded between the geometry and plate of the rheometer and allowed to equilibrate for 3 minutes at 60°C. In order to avoid excessive evaporation, a fast cooling rate of 20°C min^{-1} was applied in order to reduce the temperature to 40°C. For samples containing more than 1 wt% micro-crystalline wax, the equilibrating temperature was 80°C, and a fast cooling was subsequently applied in order to bring the temperature down to a starting temperature of 60°C. Subsequent to rapid cooling, a shear stress of 0.01 Pa was applied while cooling the sample to 4°C at rate of 1°C min^{-1}. The applied shear stress of 0.01 Pa provides near-quiescent conditions during cooling, in order to minimize the impact of shear forces during the gelation process. All gelation temperature measurements are repeated in duplicate in order to confirm experimental reproducibility.

Gelation temperature is the temperature at which the system transitions from a fluid state into a gel state. Using this method, gelation temperature is readily defined as a sharp drop, or an apparent break, in the measured shear rate curve [19].

Gel Yield Stress Determination

Sample was loaded between the geometry and plate of the rheometer and allowed to equilibrate for 3 minutes at 60°C. A fast cooling rate of 20°C min^{-1} was applied to reduce the temperature to a temperature 40°C, and then cooled at a rate of 1°C min^{-1} while continuing the cooling until 4°C. For samples containing more than 1 wt% micro-crystalline wax, the equilibrating temperature was 80°C, and fast rate was applied for cooling to 60°C. The sample was maintained at a temperature of 4°C for 10 minutes for equilibration prior to application of a shear rate of 0.1 s^{-1}. All yield stress measurements are repeated in duplicate in order to confirm experimental reproducibility.

Cross Polarized Microscopy

A Nikon Eclipse microscope ME600 in cross polarization mode was used for observing the crystal formation process and subsequent crystal morphology. A combination of 10X/22 ocular lens and ELWD 20X/0.4 objective lens provides a magnification of 200X. A VitroTube rectangular capillary sized 1 mm wide and 0.05 mm deep (Vitrocom) was used to contain the wax sample, allowing the observation at the specified temperature range. The sample and capillary were preheated at 80°C. Subsequently, the capillary was dipped into the sample to

allow the sample to fill the capillary. Both ends of the capillary were sealed with 3M Scotch cyanoacrylate base glue.

A Linkam LTS120 temperature control stage was used to regulate the sample temperature. The initial temperature was set to 80°C, and was maintained for 10 minutes after loading the sample, in order to ensure that the wax components were properly dissolved. A fast cooling of 20°C min^{-1} was applied to bring the temperature down to 60°C. Subsequently, the sample was cooled to 4°C at a rate of 0.5°C min^{-1}, and maintained for 30 minutes at 4°C. A CoolSnap-Pro monochrome digital camera from Media Cybernetics was used to capture crystal images in size of 2.4 mega pixel.

RESULT AND DISCUSSION

Waxy model oils were formulated by varying the proportion of micro-crystalline wax added to a base model oil composition containing a fixed value of 5 wt% macro-crystalline wax. The micro-crystalline wax addition ranges from 0.03 to 5 wt%, as shown in Table 1. The total wax content in solution increases with addition of micro-crystalline wax, such that the total wax content of the co-blended wax systems ranges from 5.03 to 10 wt%. Table 1 also shows the micro-crystalline fraction of the total wax as well as the ratio of micro-crystalline to macro-crystalline wax.

The wax samples are polydisperse, with a component distribution as shown in Figure 1 (a) for the macro-crystalline wax and (b) for the micro-crystalline wax. Weight average carbon number for the macro-crystalline wax is found to be C_{28}, while for the micro-crystalline one it is C_{51}.

Both waxes contain *n*-paraffin components as well as non-*n*-paraffin components. Knowing the fraction of micro- and macro-crystalline wax in each sample and the original wax composition, the composition of the wax mixture composition can be calculated. Table 1 shows the calculated percentage of *n*-paraffins and non-*n*-paraffins component in each wax mixture.

WAT Determination by DSC

DSC is a method that widely is used to define the wax appearance temperature (WAT) of wax systems[20-23]. WAT is determined as the onset point of heat flow thermogram against cooling ramp. Figure 2 illustrates the thermograms of wax in dodecane at a cooling ramp of 1 °Cmin^{-1}. Despites being polydisperse, 5 wt% macro-crystalline wax solution shows a typical strong exothermic peak due to its high crystallization enthalpy. The peak is clearly observed as the heat flow signal deviates drastically from the baseline when the wax crystalizes. The peak's height, the distance between the maximum heat flow signal at the top of the peak to the baseline, is 6 mW/g. The wax crystallization peak spans the entire temperature range starting from the crystallization onset point all the way down to the solvent solidification temperature of approximately –15 °C. The crystallization onset point of the 5 wt% macro-crystalline wax solution, determined according to the method reported by Hansen [21], is 20.5 °C.

On the other hand, 5 wt% micro-crystalline wax has a low and broad exothermic crystallization peak. Non-linear paraffins in micro-crystalline wax are more amorphous in nature and have a lower crystallization enthalpy [24]. The crystallization peak height is 3.5 mW/g. The peak is also broadened as a result of the wide component distribution of Sasolwax 3971, which spans from C_{22} to C_{80}. The crystallization onset point of 5 wt% micro-crystalline wax is found to

be 43.5 °C, which is 23 °C higher than that of macro-crystalline wax. Unlike macro-crystalline wax, the crystallization onset point determination for micro-crystalline wax is more uncertain because the heat flow signal deviates gradually from the baseline as the wax crystallizes. At lower concentrations of micro-crystalline wax, the peak is even more subtle and the onset point determination is even more uncertain.

Thermogram of 5 wt% macro-crystalline + 5 wt% micro-crystalline wax solution in Figure 2 shows an overlap of two peaks. Both peaks are shifted to higher temperature compared to the peaks found for each pure micro or macro-crystalline wax. The onset point of micro- and macro-crystalline wax crystallization are found to be 48.4 and 27.6 °C, which are respectively 4.1 and 4.9 °C higher than the original onset points of the respective neat solutions. This shift is due to a higher amount of wax content in the solution (10 wt% in total, in comparison to 5 wt% for the neat solutions). WAT is known to increase monotonically with increasing overall wax content [25]. Qualitatively, the onset point shape of the macro-crystalline wax in the mixture is found to be less sharp than the original due to peak overlapping. The baseline prior to the macro-crystalline wax onset is actually the broad body of micro-crystalline wax peak, and the tail of the micro-crystalline wax peak also contributes to the macro-crystalline wax peak itself. This result is common in polydisperse systems, where molecules of close to the same size can co-crystallize and pack together in the same crystal.

Gelation Temperature Determination by Rheometry

Gelation temperature is determined by the method of constant imposed shear stress developed by Zhao et.al [19]. This method is based on the idea that at constant shear stress, the mechanical dynamics of the system changes from flowing behavior to creeping flow over a small

temperature region in which gelation occurs. Gelation temperature measurements are repeated in duplicate. A typical shear rate vs temperature plot for 5 wt% macro-crystalline wax is shown in Figure 3. At high temperature where the solution is in liquid state, the resultant shear rate is relatively constant but varies in an Arrhenius manner with respect to temperature. Upon further cooling, the resultant shear rate transition at the gelation temperature shows a sharply decreasing trend, characterized by a sharp break in the curve driven by the well-defined gelation process. The gelation temperature is found to be 17.6 °C, about 2.9 °C below the WAT as determined by DSC, indicating that a relatively small solid fraction is required in order to form a gel from macro-crystalline wax. The small solid fraction required to form a gel from macro-crystalline wax is consistent with large aspect ratios of platelets formed from macro-crystalline wax. Applied percolation theory [26] infers that the incipient solid fraction at gelation is inversely proportional to the mean aspect ratio of the particles.

For 5 wt% micro-crystalline wax, the gelation temperature is found to be 31.4°C, about 12.1 °C below the WAT determined by DSC, indicating that a relatively high solid fraction is required in order to form a gel from micro-crystalline wax. Below the WAT, the measured shear rate decreases upon cooling, prior to declining rapidly, but not sharply, upon reaching the gelation transition temperature. This observation indicates that more precipitated wax crystals and a corresponding higher solid fraction are required in the system of micro-crystalline wax in comparison to the macro-crystalline wax, in order to form a gel. The larger solid fraction required to form a gel from micro-crystalline wax is consistent with a low mean aspect ratio of the spherical-like aggregates formed from micro-crystalline wax. Applied percolation theory infers a higher solid fraction for micro-crystalline particles at the incipient gelation point. The greater presence of wax crystals and higher solid fraction increases the apparent viscosity of the

system prior to network formation and gelation, which is manifested in a reducing shear rate upon cooling, prior to gelation, and ultimately generating a broadly sloping curve above the gelation point instead of a sharp transition at the gelation point, as in the case of the macro-crystalline wax system.

Figure 3 also shows the temperature versus shear rate profile of 5 wt% macro-crystalline + 3 wt% micro-crystalline wax mixture. The gelation temperature and measured shear rate profile are observed to be intermediate to the cases of neat macro-crystalline and neat micro-crystalline wax model systems. The gelation temperature is 22.8 °C, which is 5.3 °C higher than that of macro-crystalline wax, indicating that an intermediate solid fraction is required to form a gel from the mixed wax system. A gradual shear rate decline is observed prior to the gelation transition, and is characterized by a somewhat sharper shear rate transition than for the case of the neat micro-crystalline gel, but a less sharp transition than in the case of the neat macro-crystalline gel. The shear rate profile corroborates the intermediate solid fraction required in order to form a gel from the mixed wax system. The intermediate solid fraction at the incipient gelation point is consistent with an intermediate mean particle aspect ratio, according to applied percolation theory.

Gelation Temperature and WAT Comparison

In Figure 4 the gelation temperature of the base system of 5 wt% macro-crystalline wax in dodecane is plotted versus the micro-crystalline wax addition. At micro-crystalline wax concentrations lower than 1 wt%, the gelation temperature is not substantially influenced by the additional presence of micro-crystalline wax, even though small non-monotonic variations are apparent, suggesting competing effects. However, significant and monotonic changes are

observed at micro-crystalline wax concentration higher 1 wt%, where the total wax concentration in the solution is 6 wt% or greater. In the regime of micro-crystalline wax concentrations higher than 1 wt%, increasing amounts of micro-crystalline wax increases the observed gelation temperature in a monotonic manner.

A similar and corroborative trend is observed in the DSC crystallization onset points of macro-crystalline wax solutions with added micro-crystalline wax, which are also plotted in Figure 4. The light blue points in Figure 4 correspond to the first observed crystallization onset in the mixed wax system at various concentrations of micro-crystalline wax. This first crystallization event belongs to the micro-crystalline wax components. The black points in Figure 4 correspond to the second crystallization event in the mixed systems. The second crystallization event is attributed to crystallization of macro-crystalline wax in the mixed system. At low added concentrations of micro-crystalline wax, the peak shifts and qualitative onset shape changes are small in magnitude and appear to be stochastic. Substantial and monotonic increases in crystallization onset temperature with increasing micro-crystalline wax content are observed in the concentration regime above 1 wt% micro-crystalline wax. The increasing crystallization onset temperatures with increasing micro-crystalline wax content are attributed primarily to solid-liquid phase equilibria phenomenon, in which the solubility-limiting components originate from the macro-crystalline wax in the concentration regime below 1 wt.% micro-crystalline wax and the solubility-limiting components originate from the micro-crystalline wax in the concentration regime above 1 wt.% microcrystalline wax.

Gelation temperatures are consistently observed to be 3-4 °C below the crystallization onset point for macro-crystalline wax. A relatively small fraction of solid macro-crystalline wax is required in order for the system to form a gel. An exception appears at high concentration of

micro-crystalline wax of 5 wt% (total wax concentration of 10 wt%) where the gelation temperature is confirmed 31.6 °C, surpassing the onset point of macro-crystalline wax crystallization in the mixed 10 wt% wax system. The observed gelation point of 31.6 °C confirms that the system gels prior to the onset of macro-crystalline wax components crystallizing in the system. The gelation temperature value of 31.6 °C for the 10 wt% mixed wax system is in fact as high as the gelation temperature of the neat 5 wt% micro-crystalline wax (31.4°C). In both the mixed 10wt% system and the neat 5 wt% micro-crystalline wax system, no macro-crystalline wax has crystallized at a temperature of 31.4 °C. Therefore, the gel can also be formed by micro-crystalline wax alone, without the contribution of macro-crystalline wax, which remains primarily dissolved in the liquid phase.

Yield Stress of Formed Gels

The yield stress values of 5 wt% 5405 Sasol macro-crystalline wax gel at different shear rates were measured earlier by Paso et.al [27]. It was observed that the yield stress value were identical when measured at shear rates of 0.1, 0.01, and 0.001 s^{-1}. Zhao et.al. studied the effect of cooling rate on yield stress of the system and observed that the yield stress values decreased rapidly when the cooling rate was increased from 1 to 5°C min^{-1} [19], indicating a time-dependent process required to form wax-oil gels with a high yield strength. Following the work of these authors, a shear rate of 0.1 s^{-1} and a cooling rate of 1° C min^{-1} were used for the rheological experiments performed in this study.

Figure 5 shows plot of shear stress versus strain at 4 °C for measuring yield stress of 3 samples. Initially, at low strain value, 5 wt% macro-crystalline wax shows an elastic-like response. As the strain increases, the wax gel breaks and the measured stress decays thereby

indicating the fragmentation process of the gel [27]. The yield stress measured for 5 wt% macro-crystalline wax gel at 4°C was found to be 238.0 Pa and obtained at strain value of 0.88 %.

Neat micro-crystalline wax gels show characteristics weak gels. The measured stress is on the order of 10^0 to 10^{-3} Pa for the case of the 5 wt% micro-crystalline wax gel. An elastic-like response is not observed, even at the incipient low strain values, as no increase in the stress is observed with increasing imposed shear deformation. For example, an imposed shear strain value of 0.027 % has already caused the gel to flow, and a yield stress value can be best equated to the maximum measured shear stress of 3.2 Pa.

In Figure 5 the shear stress plot of 5 wt% macro-crystalline + 0.3 wt% micro-crystalline wax gel is also shown. An elastic-like response is observed until strain value of 0.17 % before the gel yields. It is found that addition of 0.3 wt% micro-crystalline wax decreases the yield stress to 24.2 Pa from a value of 238.0 Pa for the macro-crystalline gel without added micro-crystalline wax.

Yield stress values obtained upon addition of varying amounts of micro-crystalline wax to the 5 wt% macro-crystalline wax solution are presented in Figure 6. Three yield stress regimes are observed in the investigated range of micro-crystalline wax addition. At low concentrations of added micro-crystalline wax, up to 0.1 wt%, the yield stress remains nearly constant at a high value within the range of 230 to 287 Pa. A sudden decline in yield stress is observed when the micro-crystalline wax concentration is increased to 0.13 wt%, reducing the yield stress value to 22.5 Pa. Additional increase in the micro-crystalline wax concentration to 0.5 wt% further decreases the yield stress to 5.3 Pa, approaching the yield stress of 5 wt% micro-crystalline wax in dodecane, which is 3.2 Pa.

In the initial macro-crystalline-like regime, the concentration of micro-crystalline wax up to 0.10 wt% correspond to ratio of micro- to macro-crystalline wax of 0.02 as shown in Table 1. The micro- to macro-crystalline wax ratio for the intermediate regime stretches between 0.026 and 0.10. The starting ratio of this intermediate regime is said to be a critical ratio of micro- to macro-crystalline wax for altering the gel strength. For the case of 5 wt% macro-crystalline wax, the critical ratio is found to be 0.026, corresponding to addition of 0.13 wt% micro-crystalline wax.

Further addition of micro-crystalline wax beyond a ratio of 0.10 completely changes the system to behave like a micro-crystalline wax gel. Figure 7 presents the total composition of *n*-paraffin and non-*n*-paraffin components for the mixed wax case with a ratio of micro- and macro-crystalline wax of 0.10. Figure 7 demonstrates that with an additional presence of a small but extended distribution of branched and cyclic alkane components, the wax solution is completely unable to form a strong gel.

Cross Polarized Microscopy

In order to further study the different wax mixtures and the gels formed, samples were cooled under controlled conditions and the formed wax crystals observed between crossed polarizers. Figure 8 shows the cross polarized microscope images of waxy oil models taken at 4°C under 200X magnification. Due to the fact that wax crystals are birefringent, wax crystals appear as bright objects on a dark background under cross polarized light observation.

Wax crystal images of 5 wt% macro-crystalline wax are shown in Figure 8A, and appear as platelets. The crystals are probably formed predominantly from linear alkanes, and can be as high as 50 μm long and 5 μm wide giving an aspect ratio as high as 10:1. The crystals are spread

all over the observed two-dimensional area. The brightness of the crystals are slightly different, probably because they lie at a different depth than the microscope focus plane. This indicates that the crystals are also volume spanning all over the sample. The long crystals interlock each other to form a tightly bound three-dimensional structure. As a result, this three dimensional structure entraps the liquid solvent and enables the system to become a rigid gel with a high yield stress. The crystal interlocking is possible to occur in the process of crystal growth and co-crystallization. Kane et.al [28] hypothesized that the overlapping of growing sub-crystals leads to formation of macroscopic dimensional structures. As wax is a multicomponent system, co-crystallization ability among different n-alkanes reported by Dirand [10] and Dorset [15] is an important mechanism in this gelation process.

Figure 8B shows the microscopic image of 5 wt% micro-crystalline wax. The crystals present as irregular in shape, and crystal aggregates sized up to 20 μm appear to be formed from smaller crystal particles. The aggregates and particles spread over the samples, but do not appear to form a linking networks as found for the macro-crystalline wax sample. The existence of solid microcrystal in the system does increase the viscosity to behave like a non-Newtonian fluid, a typical property of liquid containing particles, but doesn't lead to the formation of a gel. This observation is corroborated by the rheology data in Figure 5 that the micro-crystalline 'gel' doesn't show a visco-elastic response even when a small shear force is applied.

Figure 8C shows the microscopic image of 5 wt% macro-crystalline + 0.06 wt% micro-crystalline wax mixture, representing the macro-crystalline-like yield properties regime from the rheology experiments. The crystal appearance shows no qualitative difference compared to the original macro-crystalline wax in terms of crystal size, aspect ratio, and linking network among crystals. No typical micro-crystalline wax particles are observed.

Figure 8D shows the microscopic image of 5 wt% macro-crystalline + 0.3 wt% micro-crystalline wax, representing intermediate yield properties regime from the rheology experiments. Irregular micro-crystalline wax particles and aggregates can be spotted among macro-crystalline particles. Short platelet-like crystals, typical for the macro-crystal wax, are found surrounding the micro-crystal aggregates. Apparently micro-crystalline crystallites can provide nucleation sites for more wax crystals formed further at lower temperature. Some large macro-crystals are also found separately from microcrystal aggregates, but the population is not as dense as in Figure 8A and C. The large wax crystals are also interlocked with each other, but they do not appear to bridge the entire space. Large areas are left empty as dark background, indicating an absence of birefringent material.

Figure 8E shows the microscopic image of 5 wt% macro-crystalline + 1 wt% micro-crystalline wax mixture, representing the micro-crystalline-like yield property regime obtained from the rheological experiments. It can be seen that platelet-like and irregularly shaped crystals are scattered and mixed up throughout the sample. The DSC experiments show that during the cooling, micro-crystalline crystallites are formed at a higher temperature and should occupy large volume due to their presence in large amount. Hence, only small and discrete space remains for macro-crystalline crystals to grow, forming small crystals. Interlocking among macro-crystals is spatially hindered by the presence of micro-crystalline crystallites. This mechanism is similar to the effect of recently introduced pour point depressant employing dispersible micro- and nano-particles [29-34]. As a result, the platelet-like wax crystals appear as shorter particles, having a maximum length of 10 μm and aspect ratio around 5:1, about half of the aspect ratio value found in the 5 wt% macro-crystalline wax without micro-crystalline wax.

This investigation provides a plausible mechanistic account for the known gel weakening activity of micro-crystalline wax. Addition of 0.13 wt% micro-crystalline wax into 5 wt% macro-crystalline wax solution, giving a ratio of 0.26, has been able to alter the crystal structure and leads the system to form a weaker gel as the temperature declines. This finding shows that micro-crystalline wax is a potential crystal morphology modifier for waxy oils.

Figure 9 shows a cartoon of an idealized *strong* physical gel of spherical particles, with a high specific density of inter-particle interactions. Such a gel would require a high solid fraction, due to the low aspect ratio of spherical particles. The neat micro-crystalline wax systems in the current work do not have a sufficiently high solid fraction to form a gel with elastic properties. On the other hand, Figure 10 shows a cartoon of an idealized *strong* physical gel of platelet particles, with a high specific density of inter-particle interactions. Such a gel requires a lower solid fraction, due to the higher aspect ratio of the platelets. The neat macro-crystalline wax systems in this work do have a sufficiently high solid fraction to form a gel with elastic properties. Progressive inclusion of more micro-crystalline wax into the macro-crystalline wax solution imparts a reduction in the realized aspect ratio, hindering the formation of a *strong* particulate gel, and thereby producing a weaker gel.

CONCLUSION

Waxy oil models are formulated by adding varying amounts of micro-crystalline wax into an original solution of 5 wt% macro-crystalline in dodecane. WAT of the original oil model is observed to be 20.5 °C by using DSC and the gelation temperature is determined to be 17.6 °C by using constant-stress rheometry. At an analogous concentration of 5 wt%, the micro-crystalline wax solution has a 23.0 °C higher WAT and a 13.8 °C higher gelation temperature, in

comparison to the macro-crystalline wax solution. Addition of less than 1 wt% micro-crystalline wax into a model oil containing 5 wt% macro-crystalline wax has no significant impact on the WAT or gelation temperature. A further addition of micro-crystalline wax, beyond 1 wt%, gradually increases the WAT and gelation temperature, because of the higher crystallization temperature of micro-crystalline wax. The effect of micro-crystalline wax addition upon the WAT and gelation temperature is found to be merely attributed to overlapping compositions of macro- and micro-crystalline wax.

A more significant effect of micro-crystalline wax is observed on yield stress of the gel. Addition of as low as 0.13 wt% micro-crystalline wax reduces the yield stress of waxy oil model from 238 to 22.5 Pa. Further addition of micro-crystalline wax to a concentration of 0.5 wt% reduces the yield stress to 5.38 Pa, which is very close to the yield stress of 5 wt% micro-crystalline wax gel of 3.24 Pa. Addition of micro-crystalline wax clearly reduces the strength of macro-crystalline wax gels. A critical concentration of micro-crystalline wax addition capable of altering the system to a weaker rheological state is found to be 0.13 wt%, analogous to a ratio of micro- to macro-crystalline wax of 0.026.

Microscopy images reveal two mechanisms leading to the formation of a weak gel. The first mechanism is the nucleation templating effect of micro-crystalline wax. At low to medium micro-crystalline wax concentrations, micro-crystals previously formed during cooling provide nucleation sites for subsequent precipitation of macro-crystalline wax. Macro-crystals formed in the presence of micro-crystals grow in smaller in size, the growth is localized, and the aspect ratios are reduced in comparison to the aspect ratios of neat macro-crystalline wax. The second mechanism is a special hindrance effect. Modified macro-crystalline wax precipitation leads to uneven dispersion of the macro-crystalline crystals in the liquid phase. At high concentration,

micro-crystals form throughout the sample prior to precipitation of macro-crystalline wax. Hence, only small and discrete space remains for macro-crystalline crystals to grow, forming small crystals. Interlocking among macro-crystals is spatially hindered by the presence of micro-crystalline crystallites. At this condition, the system completely behaves as a micro-crystalline gel. This investigation provides a combination of two plausible mechanistic accounts for the known gel weakening activity of micro-crystalline wax.

ACKNOWLEDGEMENTS

All authors acknowledge Thorsten Butz and Gernot Meyer, localized at Sasol Wax GmbH (Germany), for performing the HTGC analysis using a proprietary chromatography configuration and protocol. Muh Kurniawan acknowledges the Ministry of Energy and Mineral Resources of the Republic of Indonesia for financial support during his Ph.D. studies.

REFERENCES

1. Roenningsen, H. P.; Bjoerndal, B.; Baltzer Hansen, A.; Batsberg Pedersen, W., Wax precipitation from North Sea crude oils: 1. Crystallization and dissolution temperatures, and Newtonian and non-Newtonian flow properties. *Energy & Fuels* **1991,** *5* (6), 895-908.
2. Singh, P.; Venkatesan, R.; Fogler, H. S.; Nagarajan, N., Formation and aging of incipient thin film wax-oil gels. *AIChE Journal* **2000,** *46* (5), 1059-1074.
3. Kané, M.; Djabourov, M.; Volle, J.-L.; Lechaire, J.-P.; Frebourg, G., Morphology of paraffin crystals in waxy crude oils cooled in quiescent conditions and under flow. *Fuel* **2003,** *82* (2), 127-135.
4. Létoffé, J. M.; Claudy, P.; Kok, M. V.; Garcin, M.; Volle, J. L., Crude oils: characterization of waxes precipitated on cooling by d.s.c. and thermomicroscopy. *Fuel* **1995,** *74* (6), 810-817.
5. Webber, R. M., Yield Properties of Wax Crystal Structures Formed in Lubricant Mineral Oils. *Industrial & Engineering Chemistry Research* **2001,** *40* (1), 195-203.
6. Visintin, R. F. G.; Lapasin, R.; Vignati, E.; D'Antona, P.; Lockhart, T. P., Rheological Behavior and Structural Interpretation of Waxy Crude Oil Gels. *Langmuir* **2005,** *21* (14), 6240-6249.
7. Chang, C.; Boger, D. V.; Nguyen, Q. D., The Yielding of Waxy Crude Oils. *Industrial & Engineering Chemistry Research* **1998,** *37* (4), 1551-1559.

8. Paso, K. G., Comprehensive Treatise on Shut-in and Restart of Waxy Oil Pipelines. *Journal of Dispersion Science and Technology* **2014,** *35* (8), 1060-1085.
9. Venkatesan, R.; Nagarajan, N. R.; Paso, K.; Yi, Y. B.; Sastry, A. M.; Fogler, H. S., The strength of paraffin gels formed under static and flow conditions. *Chemical Engineering Science* **2005,** *60* (13), 3587-3598.
10. Dirand, M.; Chevallier, V.; Provost, E.; Bouroukba, M.; Petitjean, D., Multicomponent paraffin waxes and petroleum solid deposits: structural and thermodynamic state. *Fuel* **1998,** *77* (12), 1253-1260.
11. Dorset, D. L., Chain length and the cosolubility of n-paraffins in the solid state. *Macromolecules* **1990,** *23* (2), 623-633.
12. Pauly, J.; Dauphin, C.; Daridon, J. L., Liquid–solid equilibria in a decane+multi-paraffins system. *Fluid Phase Equilibria* **1998,** *149* (1), 191-207.
13. Garcia, M. d. C.; Carbognani, L.; Urbina, A.; Orea, M., Paraffin Deposition in Oil Production. Oil Composition and Paraffin Inhibitor Activity. *Petroleum Science and Technology* **1998,** *16* (9-10), 1001-1021.
14. Dorset, D. L.; Baugh, L. S.; Luo, J.; Shea, K. J., Rectangular Chain Packing of Methyl-Branched Paraffins: Persistence of an Interchain Interaction and Forms of Disorder. *The Journal of Physical Chemistry B* **2011,** *115* (28), 8858-8863.
15. Dorset, D. L., Crystallography of Real Waxes: Branched Chain Packing in Microcrystalline Petroleum Wax Studied by Electron Diffraction. *Energy & Fuels* **2000,** *14* (3), 685-691.
16. Zhao, Y.; Kumar, L.; Paso, K.; Ali, H.; Safieva, J.; Sjöblom, J., Gelation and breakage behavior of model wax-oil systems: Rheological properties and model development. *Industrial and Engineering Chemistry Research* **2012,** *51* (23), 8123-8133.
17. Bacon, M.; Romero-Zeron, L. B., Optimizing Paraffin and Naphthene Wax-Treatment Options Using Cross-Polarized Microscopy. In *SPE International Symposium on Oilfield Chemistry*, Society of Petroleum Engineers: The Woodlands, Texas, USA, 2011.
18. del Carmen García, M.; Carbognani, L.; Orea, M.; Urbina, A., The influence of alkane class-types on crude oil wax crystallization and inhibitors efficiency. *Journal of Petroleum Science and Engineering* **2000,** *25* (3), 99-105.
19. Zhao, Y.; Paso, K.; Kumar, L.; Safieva, J.; Sariman, M. Z. B.; Sjöblom, J., Controlled Shear Stress and Controlled Shear Rate Nonoscillatory Rheological Methodologies for Gelation Point Determination. *Energy & Fuels* **2013,** *27* (4), 2025-2032.
20. Jiang, Z.; Hutchinson, J. M.; Imrie, C. T., Measurement of the wax appearance temperatures of crude oils by temperature modulated differential scanning calorimetry. *Fuel* **2001,** *80* (3), 367-371.
21. Baltzer Hansen, A.; Larsen, E.; Batsberg Pedersen, W.; Nielsen, A. B.; Roenningsen, H. P., Wax precipitation from North Sea crude oils. 3. Precipitation and dissolution of wax studied by differential scanning calorimetry. *Energy & Fuels* **1991,** *5* (6), 914-923.
22. Elsharkawy, A. M.; Al-Sahhaf, T. A.; Fahim, M. A., Wax deposition from Middle East crudes. *Fuel* **2000,** *79* (9), 1047-1055.
23. Claudy, P.; Létoffé, J.-M.; Neff, B.; Damin, B., Diesel fuels: determination of onset crystallization temperature, pour point and filter plugging point by differential scanning calorimetry. Correlation with standard test methods. *Fuel* **1986,** *65* (6), 861-864.
24. Meyer, G., Thermal Properties of Micro-crystalline Waxes in Dependence on the Degree of Deoiling. *SOFW Journal* **2009,** *8* (135), 43.

25. Zhao, Y.; Paso, K.; Norrman, J.; Ali, H.; Sørland, G.; Sjöblom, J., Utilization of DSC, NIR, and NMR for wax appearance temperature and chemical additive performance characterization. *Journal of Thermal Analysis and Calorimetry* **2015,** *120* (2), 1427-1433.
26. Paso, K.; Senra, M.; Yi, Y.; Sastry, A. M.; Fogler, H. S., Paraffin Polydispersity Facilitates Mechanical Gelation. *Industrial & Engineering Chemistry Research* **2005,** *44* (18), 7242-7254.
27. Paso, K.; Kompalla, T.; Oschmann, H. J.; Sjöblom, J., Rheological Degradation of Model Wax-Oil Gels. *Journal of Dispersion Science and Technology* **2009,** *30* (4), 472-480.
28. Kané, M.; Djabourov, M.; Volle, J.-L., Rheology and structure of waxy crude oils in quiescent and under shearing conditions. *Fuel* **2004,** *83* (11), 1591-1605.
29. Norrman, J.; Solberg, A.; Sjöblom, J.; Paso, K., Nanoparticles for Waxy Crudes: Effect of Polymer Coverage and the Effect on Wax Crystallization. *Energy & Fuels* **2016,** *30* (6), 5108-5114.
30. Yang, F.; Yao, B.; Li, C.; Sun, G.; Ma, X., Oil dispersible polymethylsilsesquioxane (PMSQ) microspheres improve the flow behavior of waxy crude oil through spacial hindrance effect. *Fuel* **2017,** *199*, 4-13.
31. Yao, B.; Li, C.; Yang, F.; Mu, Z.; Zhang, X.; Sun, G., Effect of oil dispersible polymethylsilsesquioxane microspheres on the formation and breakage of model waxy oil gels. *Fuel* **2017,** *209*, 424-433.
32. Yao, B.; Li, C.; Yang, F.; Sjöblom, J.; Zhang, Y.; Norrman, J.; Paso, K.; Xiao, Z., Organically modified nano-clay facilitates pour point depressing activity of polyoctadecylacrylate. *Fuel* **2016,** *166*, 96-105.
33. Yang, F.; Yao, B.; Li, C.; Shi, X.; Sun, G.; Ma, X., Performance improvement of the ethylene-vinyl acetate copolymer (EVA) pour point depressant by small dosages of the polymethylsilsesquioxane (PMSQ) microsphere: An experimental study. *Fuel* **2017,** *207*, 204-213.
34. Yao, B.; Li, C.; Yang, F.; Zhang, Y.; Xiao, Z.; Sun, G., Structural properties of gelled Changqing waxy crude oil benefitted with nanocomposite pour point depressant. *Fuel* **2016,** *184*, 544-554.

Table 1. Composition of wax in dodecane solutions

Wax concentration (wt%)			Fraction of micro-crystalline[a]	Ratio of micro-crystalline[b]	Component	
Macro	Micro	Total			n-paraffin	iso-paraffin
5.00	0.00	5.00	0.00	0.0	77.6	22.4
5.00	0.03	5.03	0.006	0.006	77.2	22.8
5.00	0.05	5.05	0.010	0.01	77.0	23.0
5.00	0.10	5.10	0.020	0.02	76.4	23.6
5.00	0.13	5.13	0.025	0.026	76.0	24.0
5.00	0.15	5.15	0.029	0.03	75.8	24.2
5.00	0.30	5.30	0.057	0.06	74.1	25.9
5.00	0.50	5.50	0.091	0.1	72.0	28.0
5.00	1.00	6.00	0.167	0.2	67.4	32.6
5.00	3.00	8.00	0.375	0.6	54.7	45.4
5.00	5.00	10.00	0.5	1.0	47.0	53.0
0.00	5.00	5.00	1.0		16.4	83.6

a: percentage of micro-crystalline wax / total percentage of wax

b: percentage of micro-crystalline wax / percentage of macro-crystalline wax

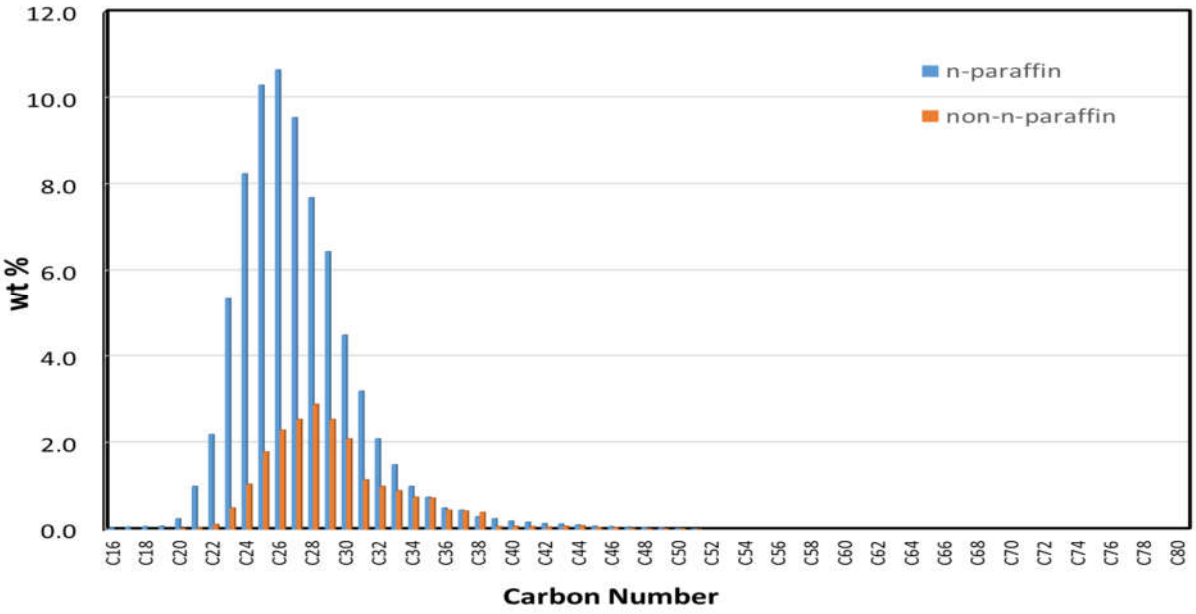
12.0
10.0
8.0
6.0
4.0
2.0
0.0
wt %
n-paraffin
non-n-paraffin
C16 C18 C20 C22 C24 C26 C28 C30 C32 C34 C36 C38 C40 C42 C44 C46 C48 C50 C52 C54 C56 C58 C60 C62 C64 C66 C68 C70 C72 C74 C76 C78 C80
Carbon Number

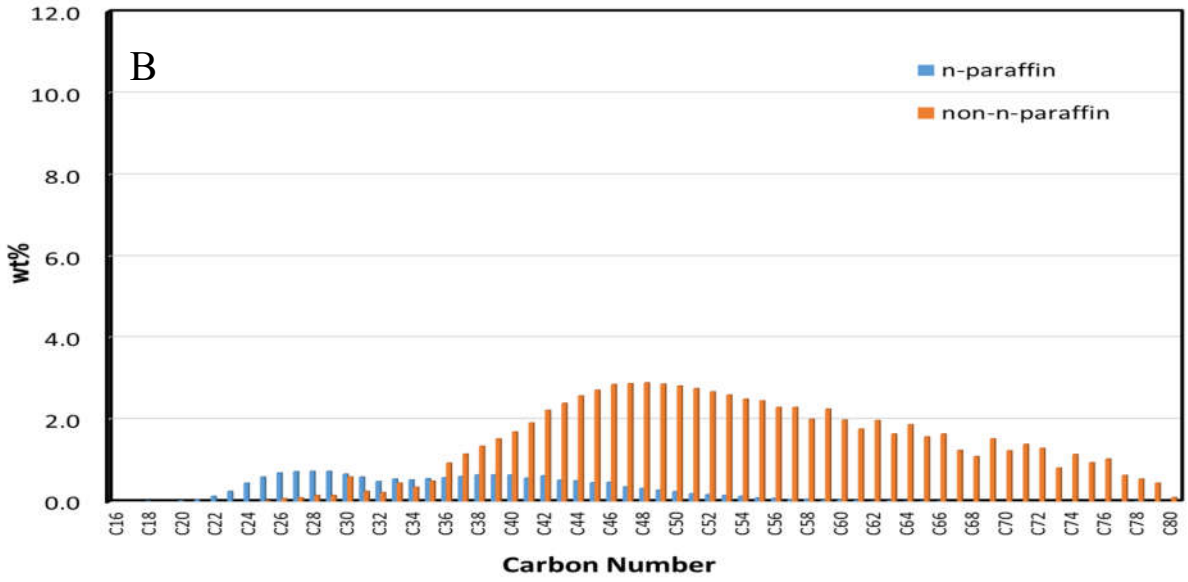
B
12.0
10.0
8.0
6.0
4.0
2.0
0.0
wt%
n-paraffin
non-n-paraffin
C16 C18 C20 C22 C24 C26 C28 C30 C32 C34 C36 C38 C40 C42 C44 C46 C48 C50 C52 C54 C56 C58 C60 C62 C64 C66 C68 C70 C72 C74 C76 C78 C80
Carbon Number

Figure 1. Component distribution of **(A)** Sasolwax 5405 macro-crystalline wax; and **(B)** Sasolwax 3971 micro-crystalline wax

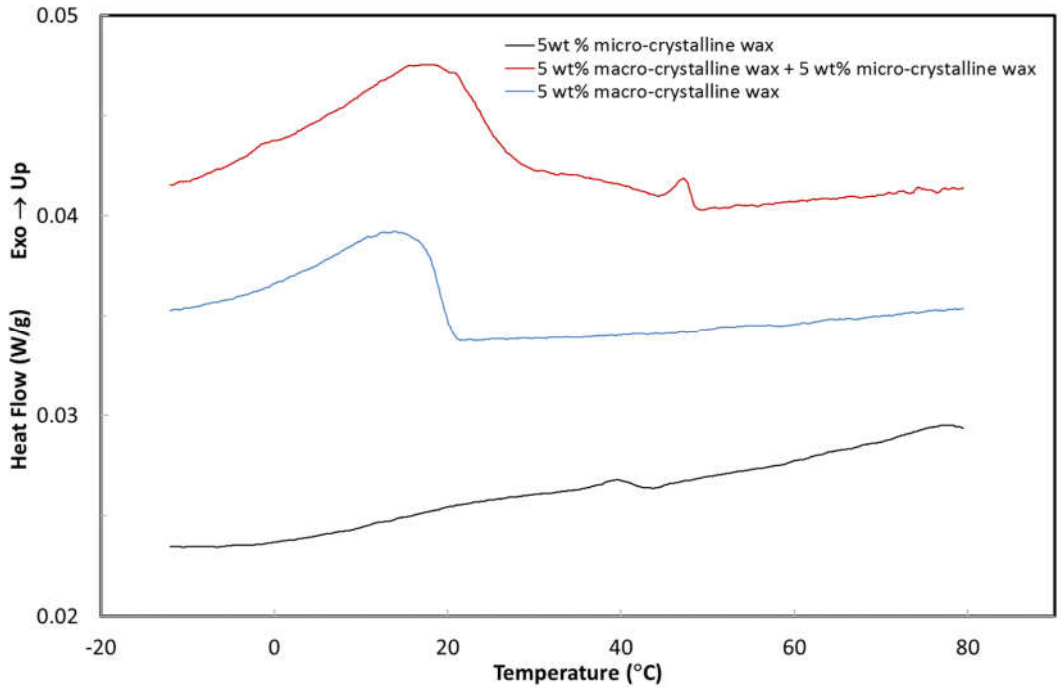

Figure 2. DSC thermogram of wax solutions in dodecane at a cooling rate of 1°C min^{-1}. Heat flow values are normalized per gram of sample.

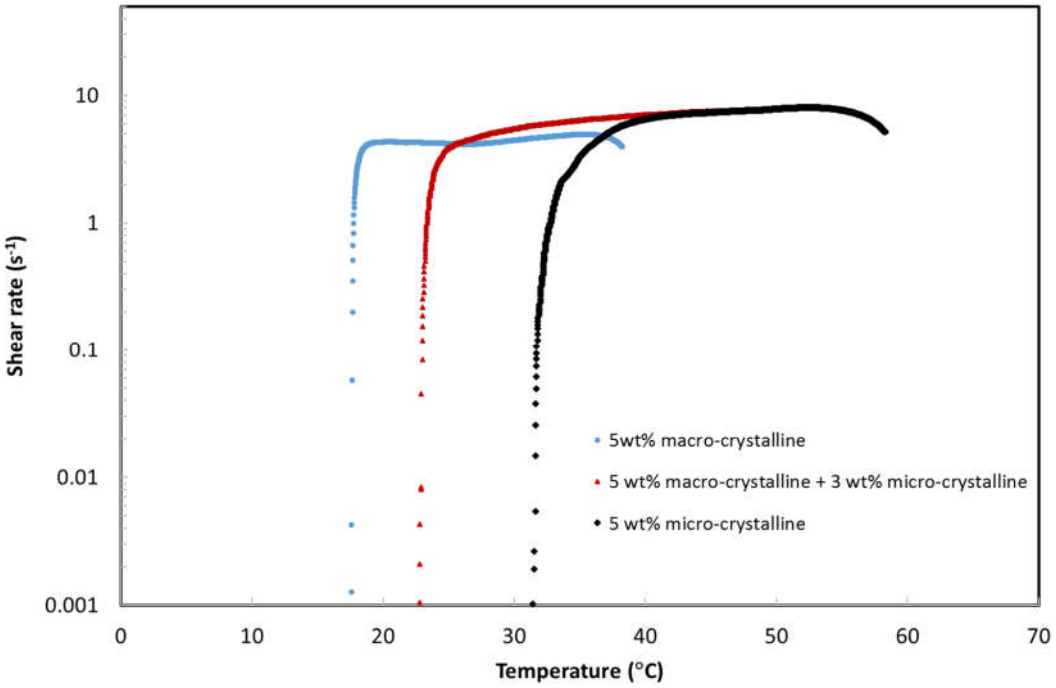

Figure 3. Shear rate of wax in dodecane versus temperature on cooling rate of 1 °C min^{-1} and controlled shear stress of 0.01 Pa for gelation temperature determination.

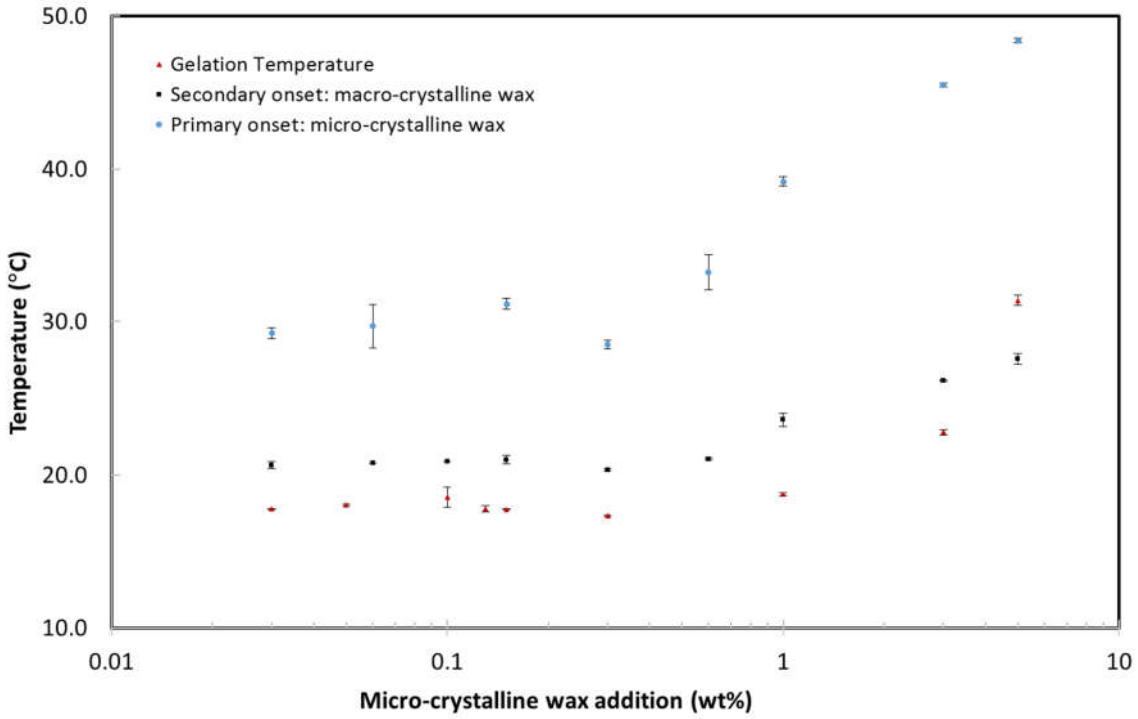

Figure 4. Gelation temperature, macro-crystalline onset point, and micro-crystalline onset point of 5 wt% macro-crystalline wax in dodecane versus addition of micro-crystalline wax. Error bars are ascribed to the uncertainty in the range of temperatures in which crystallization onset or gelation occur, based on each specific measured thermogram or rheogram, respectively.

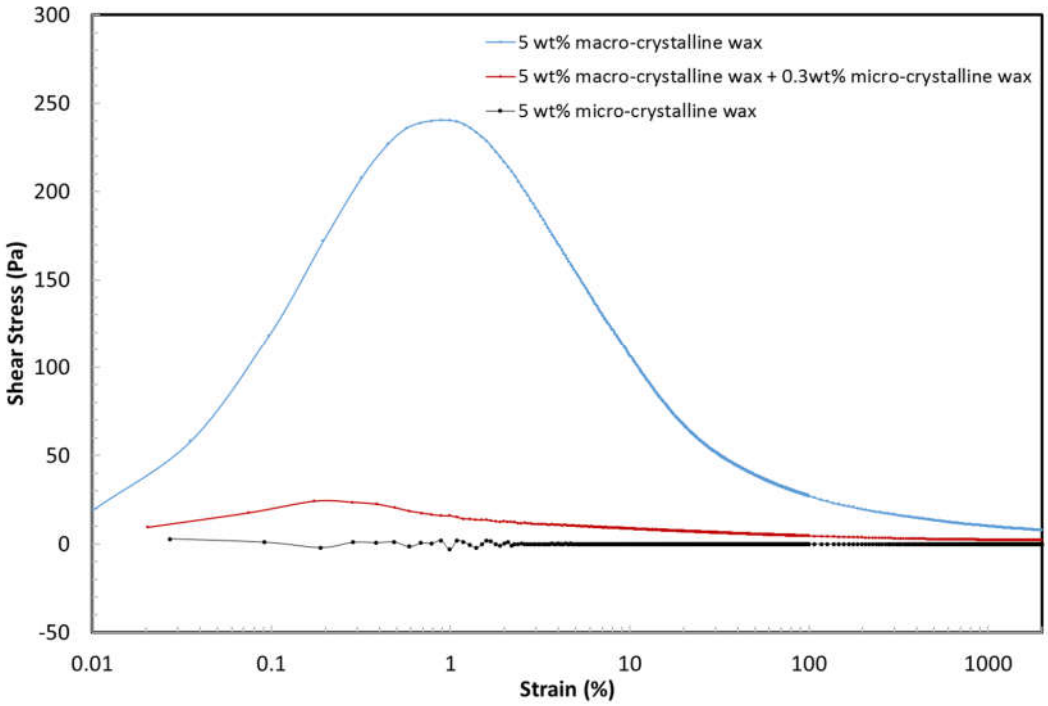

Figure 5. Plot of shear stress of wax gels versus strain at constant temperature of 4 °C for yield stress determination. The gels were formed under quiescent condition at cooling rate of 1°C min^{-1}.

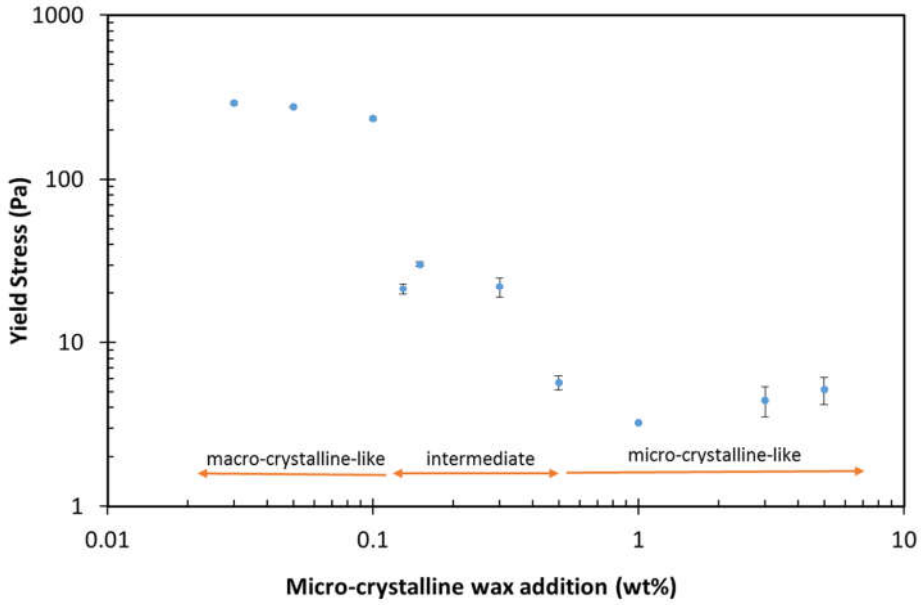

Figure 6. Yield stress of 5 wt% macro-crystalline wax gel upon addition of micro-crystalline wax.

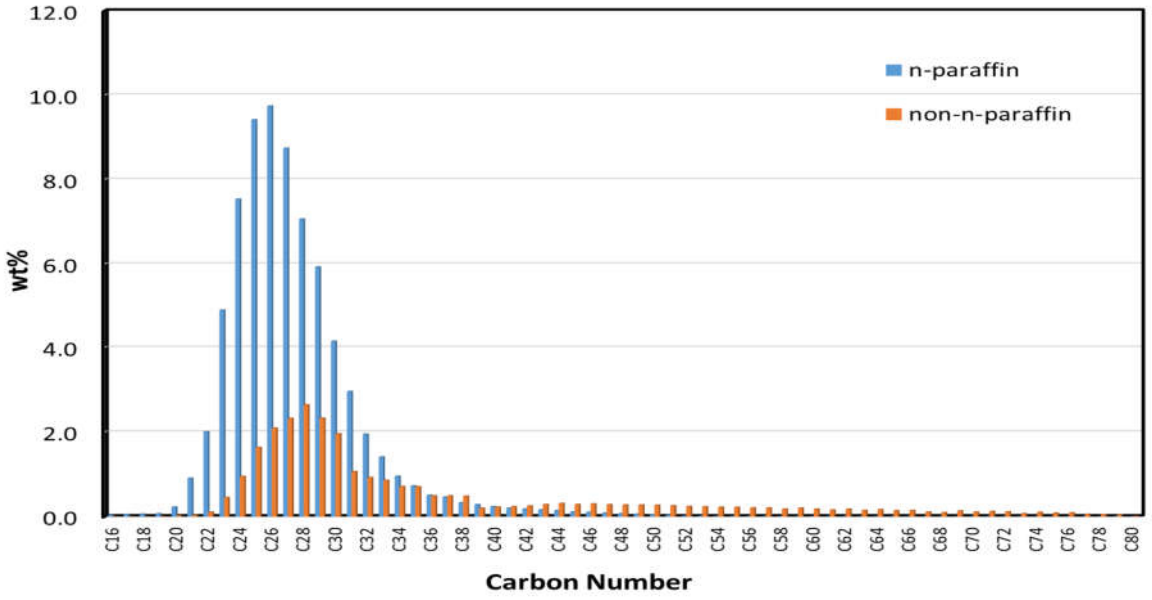

Figure 7. Component distribution of Sasolwax 3971 micro-crystalline wax and Sasolwax 5405 macro-crystalline wax mixture at ratio of 0.1.

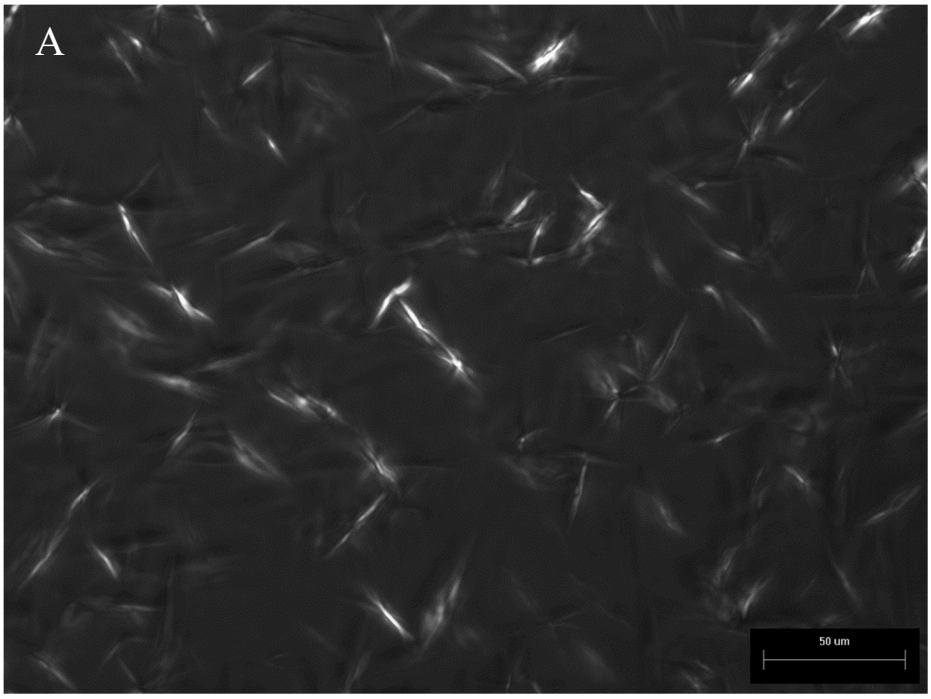
A
50 um

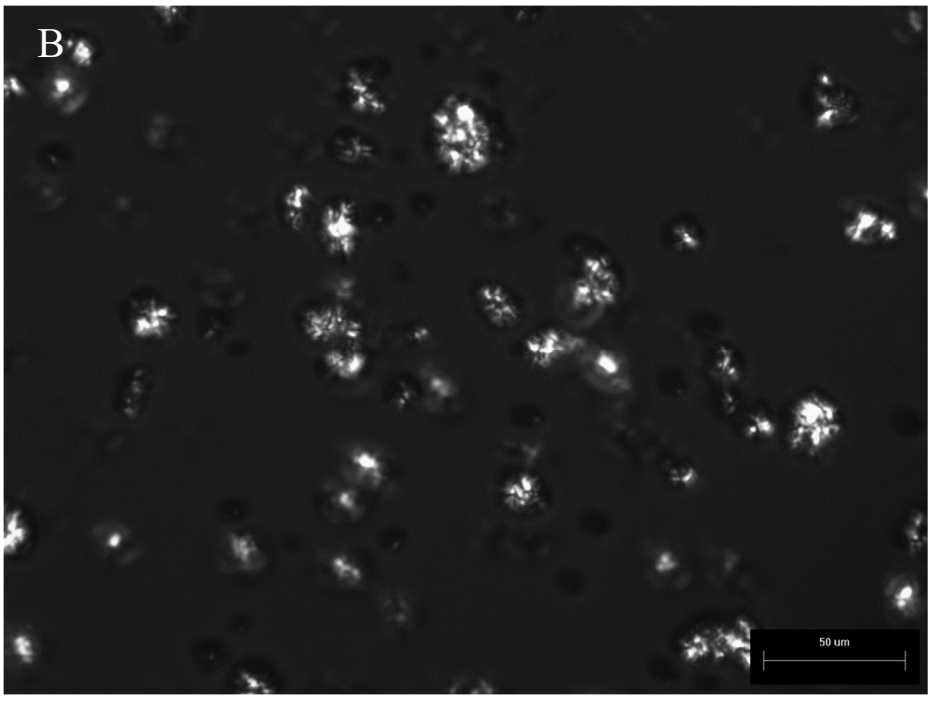
B
50 um

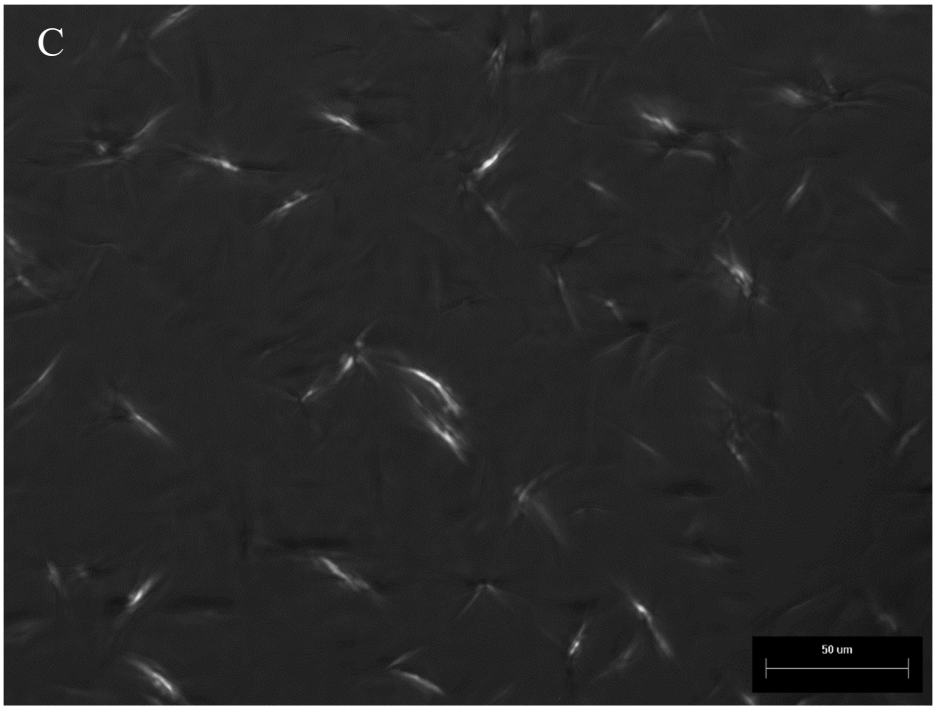
C
50 um

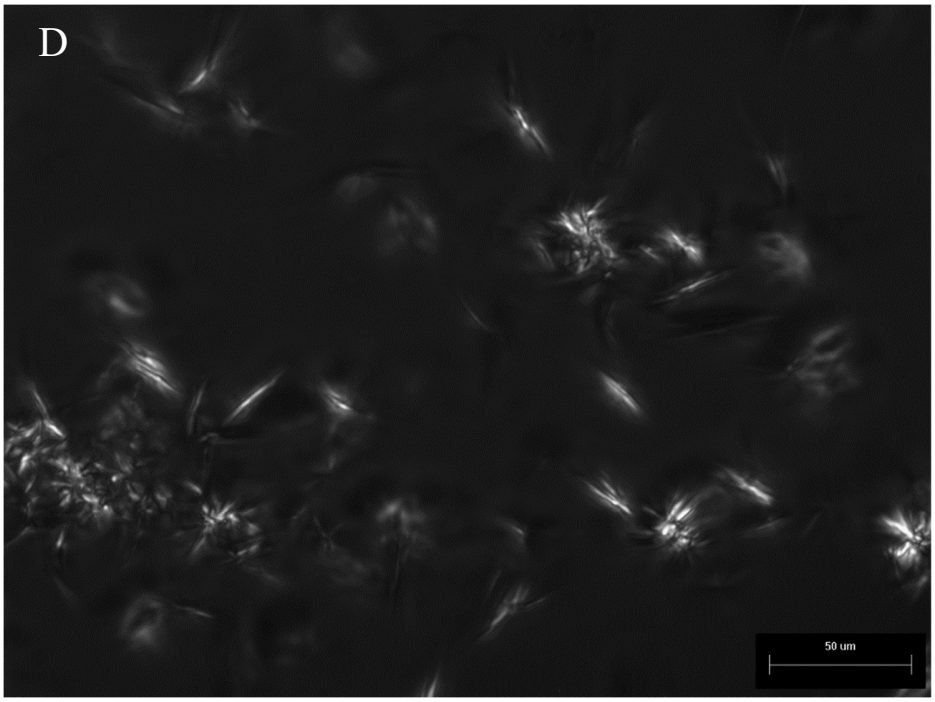
D
50 um

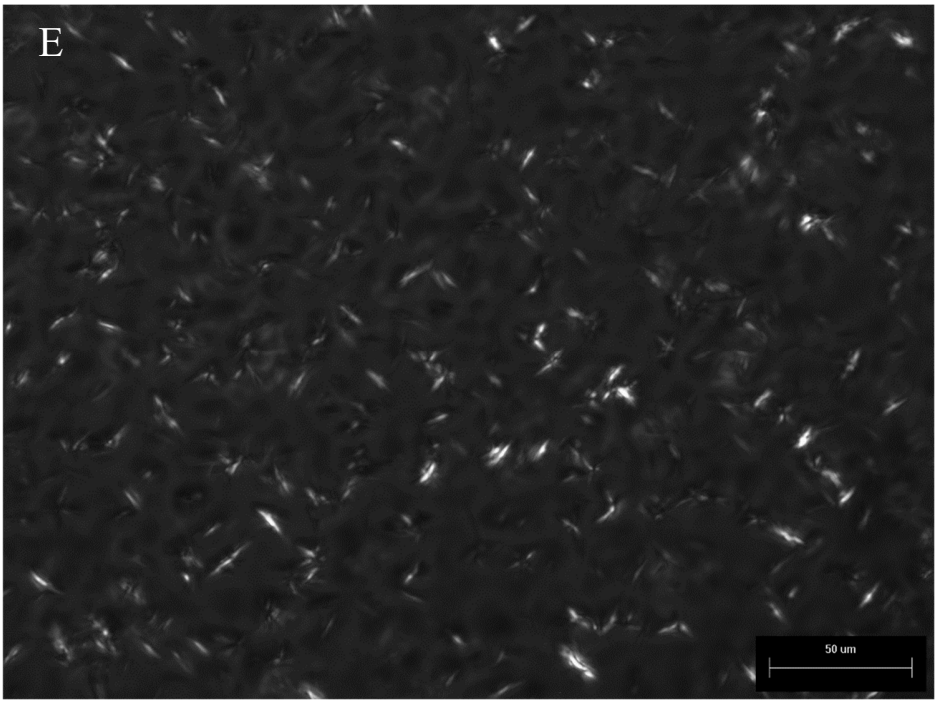

Figure 8. Cross Polarized Microscope images of wax in dodecane at 4 °C. The sample thickness is 50 μm. The measuring bar is 50 μm. **(A)** 5 wt% macro-crystalline wax; **(B)** 5 wt% micro-crystalline wax; **(C)** 5 wt% macro-crystalline + 0.06 wt% micro-crystalline wax; **(D)** 5 wt% macro-crystalline + 0.3 wt% micro-crystalline wax; **(E)** 5 wt% macro-crystalline + 1 wt% micro-crystalline wax.

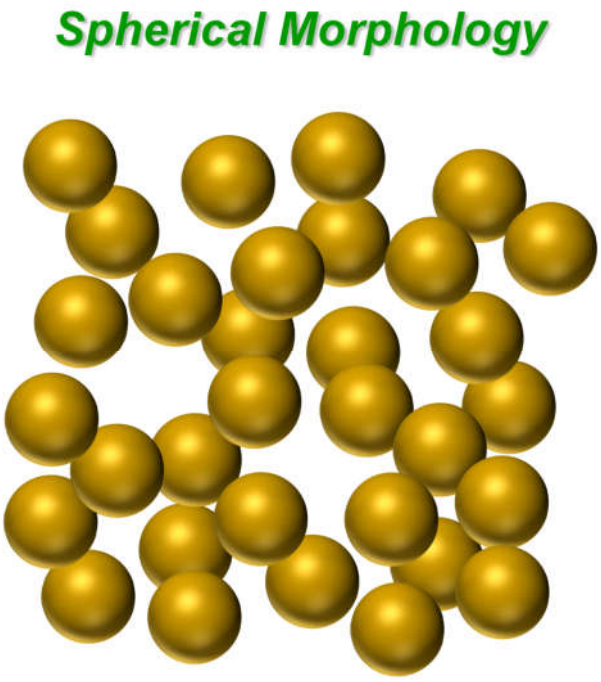

Figure 9. Idealized *strong* particulate gel of spherical particles. Because of the low aspect ratio of spheres, a high volume fraction is required to create a strong volume-spanning network of particle-particle interactions characterized by a high specific density of inter-particle interactions.

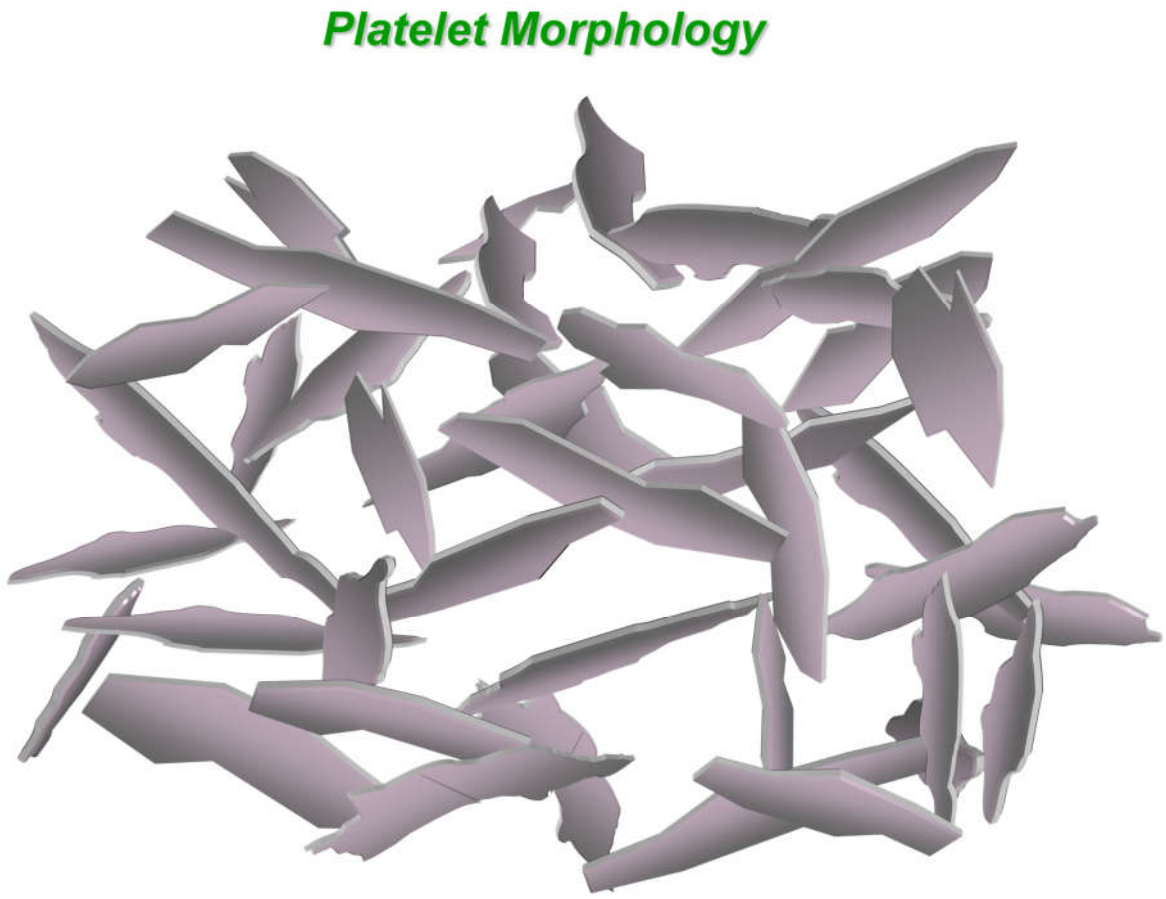

Figure 10. Idealized *strong* particulate gel of platelets. Because of the high aspect ratio, a lower volume fraction is required to create a strong volume-spanning network of particle-particle interactions, characterized by a high specific density of inter-particle interactions.